Analytica Chimica Acta xxx (xxxx) xxx

Contents lists available at ScienceDirect

Analytica Chimica Acta

journal homepage: www.elsevier.com/locate/aca

Re-engineering of peptides with high binding affinity to develop an advanced electrochemical sensor for colon cancer diagnosis

Chae Hwan Cho [a], Ji Hong Kim [a], Jayoung Kim [b, c], Jong Won Yun [d], Tae Jung Park [e, **], Jong Pil Park [a, *]

[a] Department of Food Science and Technology, Chung-Ang University, Anseong, 17546, Republic of Korea
[b] Departments of Surgery and Biomedical Sciences, Cedars-Sinai Medical Center, Los Angeles, CA, USA
[c] Department of Medicine, University of California Los Angeles, CA, 90095, USA
[d] Department of Biotechnology, Daegu University, Gyeongsan, 38453, Republic of Korea
[e] Department of Chemistry, Institute of Interdisciplinary Convergence Research, Research Institute of Chem-Bio Diagnostic Technology, Chung-Ang University, 84 Heukseok-ro, Dongjak-gu, Seoul, 06974, Republic of Korea

HIGHLIGHTS

- Electrochemical sensor for early diagnosis of adenoma-to-carcinoma progression based on rationally designed peptides.
- A series of synthetic affinity peptide was rationally designed *via in silico* molecular docking.
- More advanced site-specific immobilization of peptides on the gold surface was developed with surface chemistry approach.
- This sensor could distinguish the adenoma-carcinoma transition with improved specificity, selectivity, and stability.

GRAPHICAL ABSTRACT

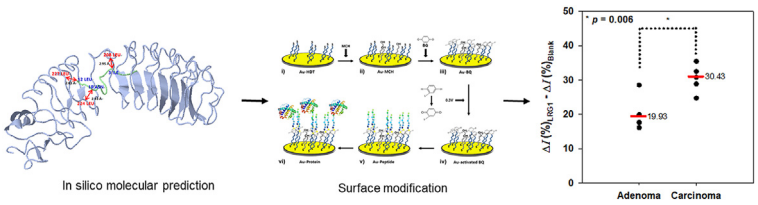

ARTICLE INFO

Article history:
Received 9 July 2020
Received in revised form
17 October 2020
Accepted 7 November 2020
Available online xxx

Keywords:
Colorectal cancer
Point-of-care diagnosis
Rational design
Molecular modeling
Electrochemical biosensor

ABSTRACT

Colorectal cancer (CRC) develops from polyps in the inner large intestine or rectum and an increasing incidence and high mortality rate has been observed in humans. Currently, colonoscopy is the preferred modality for early CRC diagnosis. However, this technique has several limitations, such as high medical costs and intricate procedures, leading to increasing demands for the development of a new, simple, and affordable diagnostic method. In this study, an advanced electrochemical biosensor based on rationally designed affinity peptides was developed for discriminating adenoma to carcinoma progression. Amino acid-substituted and rationally designed synthetic peptides (BP3-1 to BP3-8) based on *in silico* modeling studies were chemically synthesized, and covalently immobilized onto a gold electrode using aromatic ring compounds through surface chemistry techniques. The binding performance of the developed sensor system was observed using square wave voltammetry (SWV). The peptide BP3-2 was selected depending on its relative binding affinity; SWV indicated the limit of detection of BP3-2 for LRG1 to be 0.025 μg/mL. This sensor could distinguish the adenoma-carcinoma transition with improved binding abilities (specificity and selectivity), and stability in plasma samples spiked with LRG1 and real samples

Abbreviations: CD, Circular dichroism; LOD, Limit of detection; SWV, Square wave voltammetry.

* Corresponding author.
** Corresponding author.
E-mail addresses: tjpark@cau.ac.kr (T.J. Park), jppark@cau.ac.kr (J.P. Park).

https://doi.org/10.1016/j.aca.2020.11.011

from patients with CRC. These results indicate that this electrochemical sensor system can be used for early monitoring of the colorectal adenoma to carcinoma progression.

1. Introduction

Colorectal cancer (CRC), a malignant tumor found in the large intestine or rectum, is one of the most common cancers and the fourth leading cause of cancer-related death [1–4]. In recent times, there has been a significant reduction in the survival and treatment success rates of CRC [5,6] owing to early diagnosis. A statistical analysis revealed that adenocarcinoma was found to constitute 95% of all CRCs and that the transition of adenoma to carcinoma is the most critical process in CRC development [7]. CRC could also be effectively controlled and curable if the premalignant lesion (adenoma) is detected and removed before invasion. Currently, several clinical diagnostic methods are used for CRC. Among these methods, colonoscopy is considered the gold standard for early CRC diagnosis [8–10]. However, a substantial proportion of patients may find colonoscopy inconvenient due to the high medical cost and the uncomfortable procedure [11–13]. Therefore, because of increasing demands for the development of a cost-effective and reliable diagnostic method, alternatives such as DNA analysis, determination of carcinoembryonic antigen levels, and antibody-based assays have been suggested [13–17]. In particular, these methods can distinguish patients with CRC from healthy controls but cannot distinguish precancerous adenoma and carcinoma, which is crucial for early CRC diagnosis. Further, although these methods seem simpler and more affordable, a more sensitive diagnostic technology needs to be developed to distinguish precancerous adenoma and carcinoma.

Leucine-rich α-2-glycoprotein-1 (LRG1) plays a major role in apoptosis and cell survival in patients with CRC [1]. In particular, previous studies have confirmed that LRG1 expression levels in the plasma from patients with carcinoma were more than 2-fold higher than those in the plasma samples of patients with adenoma [1]. These results suggest that LRG1 is related to the transition from adenoma to carcinoma. Currently, an antibody-based detection assay is the most widely used method for detecting LRG1. Antibodies serve as important capture reagents in several fields such as the clinical or pharmaceutical analysis, diagnosis, and treatment of various diseases. However, they have limitations such as being relatively large in size and having cross-reactivity in immunoassay tests. Additionally, because most antibodies are produced in mammalian cells, they can require relatively long times for mass production, and are expensive. In contrast, affinity peptides have a small size and simple structure and are relatively stable in a variety of environmental conditions. Therefore, affinity peptides are gaining increasing attention over conventional affinity reagents in many fields [18,19].

Phage display is one of the most optimized assays for screening and/or identifying high affinity peptides for wide use in many applications such as diagnosis, small molecule-based drug development, drug delivery, and pharmaceutical analysis [16,20–25]. Newly screened peptides or proteins are used for protein-protein or protein-peptide interactions and for identification of sequences specific to their target for replacing affinity reagents that specifically bind to target proteins or metals [26,27]. Researchers have developed a peptide-based sensor capable of recognizing and capturing norovirus [28], procalcitonin (PCT) [27], and neutrophil gelatinase-associated lipocalin [29] using a combination of phage display technology and electrochemical analysis. For example, electrochemical-based biosensors have been widely applied in many fields because they have high sensitivity, are easy to control, and allow for label-free detection and miniaturization in a point-of-care setting [30–32]. Furthermore, the working electrode surface of an electrochemical sensor can be composed of many materials such as gold, silver, and graphene, and the immobilization of target-specific probes such as DNA, antibody, and protein on the working electrode surface can enable targeted specific detection in electrochemical analysis. Because of these characteristics, electrochemical biosensors stand out for extensive development toward point-of-care diagnostics [13,33–35]. Among electrochemical sensing methods, square wave voltammetry (SWV)-based detection has been widely used for the quantitative detection of various compounds such as drugs, biomolecules, and environmental pollutants. SWV has advantages such as short analysis times, simplicity, high sensitivity, and cost-effectiveness compared to other modes of analysis.

In a previous study, we screened short linear affinity peptides specific for LRG1 protein using phage display technology and evaluated their binding affinities by electrochemical analysis [22]. We then selected the best affinity peptides containing positive charges (His) or negative charges (Asp) and confirmed that they can be used to detect their target proteins in actual patient samples. Despite these successful results, the direct immobilization of short peptides on a gold electrode can sometimes lead to instability as it does not control the densities per gold surface area, and thus more optimized sensors are needed for real testing.

Considering these findings, in this study, we used a rational design approach with *in silico* modeling and synthesized advanced affinity peptides for an electrochemical sensor. In addition, a new linker was used to specifically immobilize the affinity peptide on a gold electrode with a surface chemistry approach. Finally, we tested the performance of this advanced sensor system in distinguishing patients with adenoma from those with carcinoma.

2. Materials and methods

2.1. Chemicals

Recombinant full length human leucine-rich alpha-2-glycoprotein1 (LRG1) was purchased from Origene (TP306780, Rockville, MD, USA). KNO_3, 1,6-hexanedithiol (HDT) 6-mercaptohexanol (MCH), benzoquinone, and human plasma were purchased from Sigma-Aldrich (St. Louis, MO, USA). All amino acid-substituted synthetic peptides (LRG1 BP3-1 to LRG1 BP3-8) were chemically synthesized (>95% purity) by Peptron (Daejeon, Korea) (Table S1). The commercially available LRG1 ELISA detection kit was purchased from Immuno-Biological Laboratories (cat no: 27,769, Gunma, Japan).

2.2. Circular dichroism (CD) spectroscopy

Circular dichroism spectra were carried out using a JASCO J-1500 spectropolarimeter at Korea Basic Science Institute. CD measurements were performed at 298 K using a quartz cuvette of 0.1 cm path length. The peptide sample concentration was 50 μM. The spectra were recorded from 260 nm to 190 nm, averaged three

scans. Data was recorded at a scan speed of 200 nm/min, bandwidth of 1.0 nm, 1 s response and 0.1 nm resolution., as reported previously [31].

2.3. Immobilization of the affinity peptides

The bare gold electrode was soaked in 100% ethanol (HPLC grade) for 5 min to remove residual dust and was then washed using distilled water. After that, the electrode was immersed into piranha solution (H_2SO_4:H_2O_2 = 7:3, v/v) for 10 min. After washing briefly, the electrode was soaked in 1 mL 1,6-hexanedithiol (HDT) for 3 h at 25 °C. After the required washing steps, the electrode was further immersed in 1.0 mM of 1,6-mercaptohexanol (MCH) for 1 h, the un-functionalized region on the gold surface was blocked, and then benzoquinone (BQ) was introduced on the HDT-activated gold electrode for 2 h. The pre-functionalized electrode was then dried for several seconds using N_2 gas. Next, the gold electrode was assembled with a home-made electrochemical cell; 75 μL of synthetic peptides (10 μg/mL) were introduced onto the gold electrode, and incubated for 1 h at 25 °C. To remove the unbound peptides or residual other components, the cell was washed with 0.1 M PBS buffer (pH 7.4) and pure water. Finally, 50 μL of LRG1 protein or human plasma spiked with the protein were dropped on a gold electrode and the electrochemical signal was measured after incubation.

2.4. SWV

The general electrodes, including the platinum counter electrode, Ag/AgCl reference, and working electrode (5 mm in diameter with a geometrical area of 19.6 mm^2), were used for electrochemical analysis (CH Instruments, Austin, TX). SWV measurement was conducted from −0.8 V to +0.4 V *vs*. an Ag/AgCl electrode (Ag/AgCl/1.0 mol/kg KCl vs. NHE, +0.235 V) at a frequency of 5 mV/s and 5 mV amplitude with scan increments of 4 mV. Statistical analysis of SWV experiments was based on the relative current change (ΔI %), which was calculated by comparing the current change before and after incubation of LRG1 protein with the synthetic peptide-tethered gold electrode.

$$\Delta I\ \% = (I_b - I_a)/I_b \times 100 \text{ [34]}$$

where I_b is the mean value of current in the peptide-immobilized electrode (no addition of target protein, plasma samples), and I_a represents the current after sample (target protein, plasma samples) incubation.

2.5. Quantitative analysis of LRG1 spiked in human plasma

Commercial plasma was purchased from Sigma-Aldrich. The plasma sample was then diluted with distilled water. Various concentrations of LRG1 were spiked in the plasma sample. For comparison, the LRG1 concentration was calculated based on the value of ΔI obtained by comparing the current before and after incubation with the LRG1 protein spiked in the plasma. The increased ΔI was calculated as the recovery concentration of LRG1 protein using a standard curve of SWV.

2.6. Patient samples

A total of 10 patients with adenomas and carcinomas were enrolled. In detail, blood samples from the two groups were collected and crude blood plasma was separated by centrifugation (3000×*g*, 10 min), as reported previously [1] and kept in refrigerator (−80 °C) for further analysis.

2.7. SEM

The surface morphologies of the functionalized gold electrodes were characterized by FE-SEM (SIGMA instrument from Carl Zeiss, Cambridge, UK).

2.8. Statistical analysis

Two-way and one-way analysis of coefficient of variance (COV) was performed to determine the statistical significance of the results obtained with the binding affinity peptides (GraphPad, CA, USA).

3. Results and discussion

3.1. Re-design and synthesis of affinity peptides for advanced characteristics

As mentioned earlier, we have reported the development of an affinity peptide specifically binding to LRG1 protein, a biomarker of colon cancer [3]. In that study, the affinity peptide specific to LRG1 protein had the sequence QDIMDLPDINTL, with a Cys residue at the C-terminus for binding the gold surface and a flexible linker (-GGGGS-) for flexibility. This suggested a possibility for the diagnosis of colon cancer, however, there were some hurdles to be crossed. First, the density of peptide binding with the Au-cysteine interaction on the gold electrode could not be controlled resulting in chip-to-chip variation, which resulted in low reproducible outcomes. Therefore, a more reproducible and controllable sensor layer was needed. Second, it was necessary to make a peptide with improved stability, because this is one of the critical properties required for application in actual point-of-care testing. To address these considerations with the development of a more advanced electrochemical sensor, we tried to re-design affinity peptides through *in silico* modeling studies and chemically synthesized 8 peptides (LRG1 BP3-1 to BP3-8). Based on the prediction of binding site and/or the contact map between LRG1 protein and the first version of LRG1 BP3 with *in silico* CABS-dock simulation (http://biocomp.chem.uw.edu.pl/CABSdock/), we re-built a series of peptide derivatives (Figs. S1 and S2). The sequences of the re-designed synthetic peptides and their characteristics are listed in Table S1. LRG1 BP3-1 was designed to investigate the effect of D-form amino acids on the binding interaction. In the sequence, the polar amino acids, Gln at position 1, Asp at the position 8, and Leu at position 12 were substituted with D-form amino acids. LRG1 BP3-2 and LRG1 BP3-3 were synthesized by incorporating a non-fouling peptide and a flexible linker in a 12-mer peptide specific for LRG1, respectively. Next, we synthesized LRG1 BP3-4, which has two repeats of the LRG1 specific 12-mer peptide, and LRG1 BP3-5, which has repeats of the 12-mer portion of LRG1 BP3-1 containing the D-form amino acid. Finally, LRG1 BP3-6 to 8 were prepared by replacing mini PEG2 with a flexible linker used in the above peptides.

3.2. Surface modification

As mentioned earlier, based on the principles of surface chemistry (Fig. 1), the functionalized gold sensor was created as shown in Fig. 2a. After successful manipulation, the affinity peptide-tethered gold electrode was evaluated for use as an electrochemical peptide sensor (Fig. 2, Fig. S3). The SEM images showed several peptide dots and/or clumps on the gold surface, indicating successful peptide incorporation. The change in current at each step is shown in Fig. 2b. The current reduction of the gold surface coated with MCH indicates that the non-bonded surface sites on the gold surface was saturated after HDT treatment [36]. MCH can fill the void area on

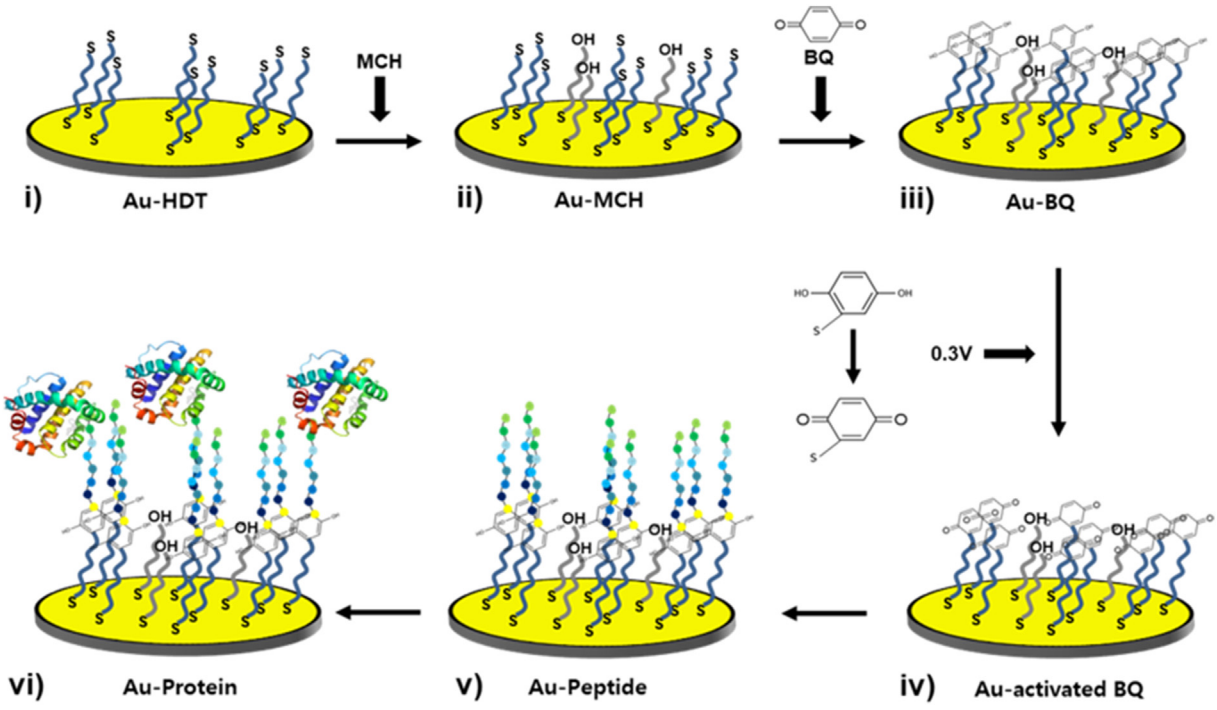

Fig. 1. Schematic illustration of surface modification. The gold electrodes were rinsed with pure water and exposed to HDT and subsequent addition of MCH for backfilling. After this step, BQ was introduced to further functionalize gold electrode, and the binding of LRG1 protein on peptide-immobilized gold surface was detected with SWV measurement.

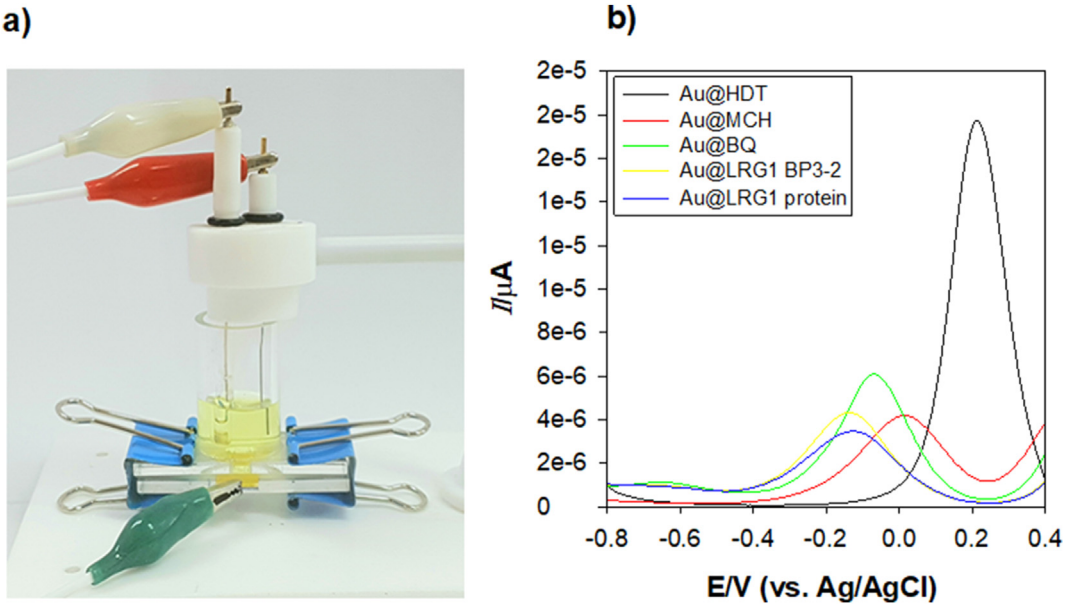

Fig. 2. The photograph of developed sensor used in this study (a) and measurement of current change during surface modification (b).

the gold surface to align HDTs and this was attributed to reduce the non-specific binding of target proteins. After proper arrangement of HDT-MCH with benzoquinone on the gold surface, the current value was increased as expected. Benzoquinone consists of a benzene ring, which facilitates the spread of electrons. Therefore, it is possible to amplify the electrochemical signal, which enhances sensitivity, resulting in the current increase when the benzoquinone was introduced on the electrode. After making the functional gold sensor layer, we compared the binding capacity of the peptide candidates with the protein by comparing the peptide values of each candidate group with the decreasing current value during the process of sequentially binding the target (LRG1 protein) (Fig. 2b). In general, most of protein or peptide act as an insulator because of their blocking of the electron transfer kinetics. Therefore, when the gold electrode was coated with an insulator, the transport of the redox could inhibited and decreased the current [37,38].

3.3. Secondary structure analysis of the synthetic peptides

To investigate the structure of the peptides and its function in

the binding interaction, CD spectroscopy was carried out. The CD spectrum of LRG1 BP3-1 showed a unique structure different from that of other peptides, and it also significantly differed from that of the first version of LRG1 BP3 (Fig. 3). LRG1 BP3-3 has one additional flexible linker and it has fewer β sheets in its structure, whereas LRG1 BP3-2 had a slightly higher number of β-sheets than LRG1 BP3-3. LRG1 BP3-4 and LRG1 BP3-5 were characterized by a large number of similar amino acid repeats and exhibited similar structures. LRG1 BP3-6 was synthesized by replacing the flexible linker in the sequence of LRG1 BP3-4 with mini PEG2. A significant increase in α-helices and a sharp decrease in β-sheets was observed in LRG1 BP3-6. PEG was incorporated in the sequence to create LRG1 BP3-7, and the only difference between this peptide and LRG1 BP3-8 was the presence and absence of a flexible linker. Like the previously mentioned LRG1 BP3-2 and LRG1 BP3-3, the two structures are very similar, and the addition of the flexible linker resulted in an increase in the β-sheet structure.

3.4. Selection of the highest affinity peptide for the detection of LRG1 protein

SWV experiments were performed in order to select the best peptide with the highest affinity for the LRG1 protein. Each synthetic peptides (10 μg/mL) were separately immobilized on the functionalized gold surface, washed 5 times with pure water and then observed the current change for fine tuning and stabilization of the gold electrode. As shown in Fig. S4, little current change in all peptides was observed, suggesting similar and successful surface functionalization. After confirmation and stabilization of the gold electrode, 1.75 μg/mL of LRG1 protein was introduced to study the relative binding affinities. In this process, the change in the current value was statistically calculated and expressed as the Δ*I* value. As shown in Fig. 4a, LRG1 BP3-1 in which L-form amino acids were substituted with D-form amino acids, exhibited a relatively low signal. In our experiment, the structural change caused by the substitution of L-form amino acids with D-form amino acids showed a negative effect on the binding to the LRG1 protein. From the observations, LRG1 BP3-2 had the highest binding affinity among the peptides tested. The effect of sequence repetition on binding was studied using LRG1 BP3-4 and LRG1 BP3-5, which contained repeating sequences of LRG1 BP3 and LRG1 BP3-1, respectively. Interestingly, LRG1 BP3-4 and LRG1 BP3-5 had different sequences but showed similar results in SWV. However, the results of LRG1 BP3-5 had a larger error value than that of other peptides. This could be a result of the non-specific bonds between the peptide and the target. As mentioned above, the substitution of L-form amino acids with D-form amino acids in LRG1 BP3-1 showed a low Δ*I* value. LRG1 BP3-6 to 8 were synthesized by incorporating mini PEG and the effect of spacers on binding affinity was also evaluated. The shape and orientation of the synthetic peptides attached to the solid surface are important for the detection of analytes, which can be influenced by spacers. LRG1 BP3-6 and LRG1 BP3-8 showed relatively high levels of binding affinity, whereas LRG1 BP3-7 showed the lowest level of binding affinity. LRG1 BP3-6 and LRG1 BP3-8 have an intermediate linker between the mini PEG and the binding site, while LRG1 BP3-7 does not. Therefore, the binding site of the 12-mer peptide specific for LRG1 protein in LRG1 BP3-7 may be affected by the relatively long mini PEG. Consequently, LRG1 BP3-2, which was tagged with non-fouling peptides, was selected due to the highest binding affinity (Fig. 4a). For confirming the selectivity of the best peptides, well-characterized proteins involved in the adenoma to carcinoma transition were used. In fact, we confirmed that bovine serum albumin and transthyretin (TTR) proteins have an equal value as the control, and that α-2-HS-glycoprotein (AHSG) has the highest value among the tested proteins. In a previous study [1], AHSG showed 30% similarity to LRG1 and is particularly similar to the peptide binding site predicted through molecular docking simulation (Fig. 4b and Fig. S2.). Based on these observations, we selected LRG1 BP3-2 as the best affinity peptide, because it had lower non-specific binding whereas its specific binding for LRG1 protein was relatively higher (Fig. 4b).

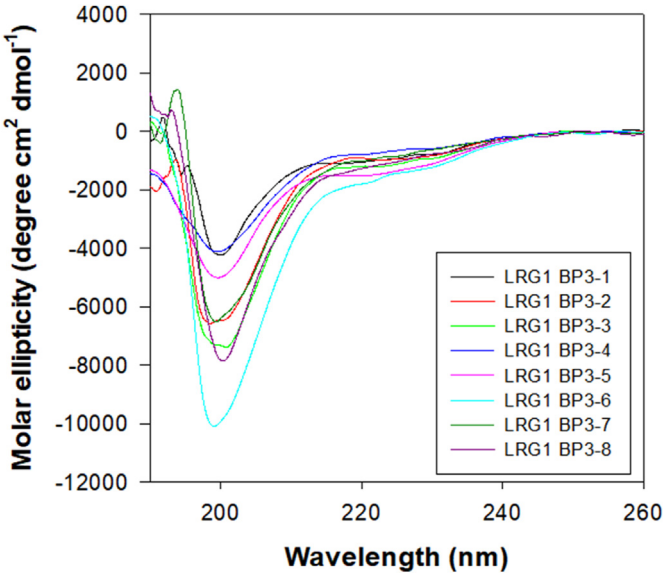

Fig. 3. Circular dichroism (CD) spectral analysis for studying the secondary structures of the synthetic peptides (50 μM).

3.5. Optimization of peptide concentration for the binding interaction

After selecting LRG1 BP3-2 as the final peptide, we conducted SWV measurements to investigate the effects of peptide concentration on the binding interactions. Peptides at various concentrations ranging from 1 to 100 μg/mL were immobilized on the gold surface and reacted with LRG1 (1.75 μg/mL). The change in current at each step was represented by Δ*I* through statistical calculations (Fig. 5a). As the peptide concentration increased, the current value was decreased gradually (Fig. S5). However, the average value of Δ*I* after reaction with LRG1 protein increased sequentially at concentrations ranging from 1 to 50 μg/mL but was decreased after reaching a saturation point at 50 μg/mL (Fig. S6). It was reported that there are some binding forces in peptide and protein interaction including van der Waals, hydrogen bond, and structural bond [36,37]. The binding force can be increased in proportion to the peptide concentration and no longer increased at saturation concentration. Therefore, we chose 50 μg/mL as the optimal concentration of the LRG1 BP3-2 peptide for further experiments. LRG1 protein at a concentration of 0–5 μg/mL was incubated on the gold surface on which 50 μg/mL of LRG1 BP3-2 peptide was immobilized, and SWV was carried out (Fig. 5b, Fig. S6). It was confirmed that the Δ*I* value continued to increase with increasing protein concentration.

3.6. Determination of binding constant and sensitivity test

As shown in Fig. 5c, the Δ*I* of LRG1 at various concentrations was plotted to determine the dissociation constant (K_d). The K_d of the best peptides was observed to be 0.1162 μg/mL (3 nM) using the following equation;

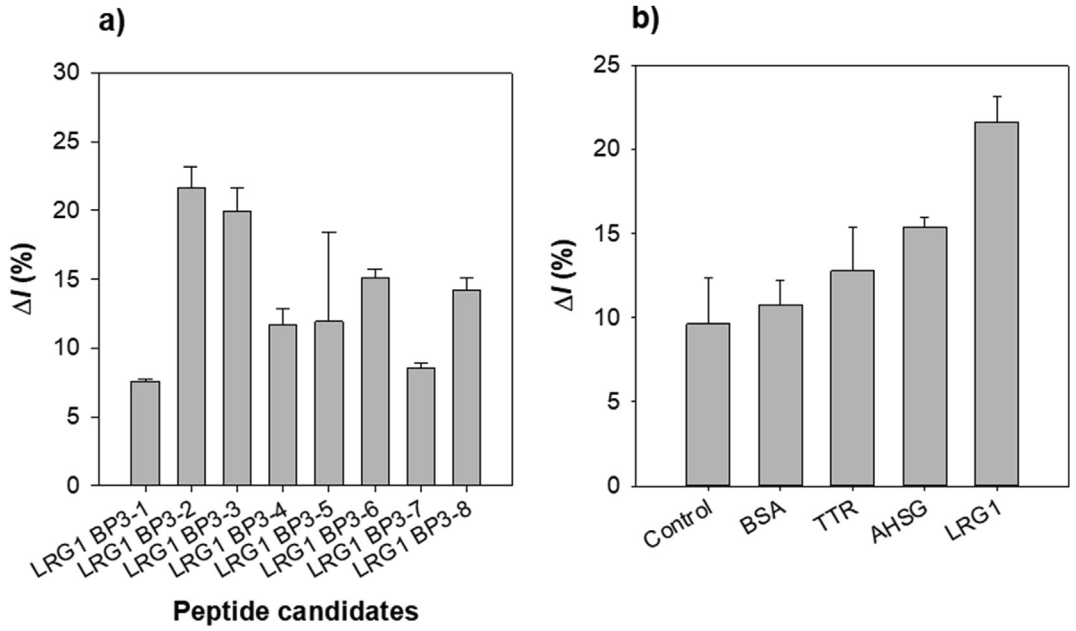

Fig. 4. Selection of potential affinity peptides. All synthesized peptides (LRG1 BP3-1 to BP3-8) were immobilized on the gold surface and their binding affinities for LRG1 proteins were evaluated using SWV (a). After screening, LRG1 BP3-2 was selected as the potential binding peptide based on its affinity compared with different proteins and the control (b). All measurements were taken in triplicate; error bars represent standard deviations.

$y = 74.02964x + 0.5824$ ($R^2 = 0.885$)

where x (μg/mL) is the concentration of LRG1, y is the value of Δ*I*. In the lower concentration range (segment 1), a large slope from the standard curve was derived from larger binding between LRG1 and the peptide. This is a rather interesting result because the re-designed affinity peptides had nanomolar affinities for LRG1 proteins, and this value was much lower (2.5-fold) compared to our previous report. We assumed that the binding affinity of the engineered peptides can be improved by molecular modeling and structure-to-function studies. Thus, the difference in the slope of the two equations can be attributed to the detection capability at low and high concentrations of LRG1. The limit of detection (LOD) was calculated as follows.

$LOD = 3 \times \sigma/S$ [29]

where σ is the standard deviation, and S is the slope of the graph with values 0.6105 (constant) and 74.0296, respectively. Based on this equation, the LOD value was found to be 0.025 μg/mL.

3.7. Stability and reproducibility

To evaluate the stability of the developed sensor, the gold electrode immobilized with the LRG1 BP3-2 (50 μg/mL) peptide was kept in 0.1 M PBS buffer (pH 7.4) at 4 °C with for up to 48 h. After storage, the pre-functionalized electrodes were removed at different time intervals, dried at room temperature for about 15 min, and reacted with 1.75 μg/mL of LRG1 protein. Interestingly, the Δ*I* values were slightly decreased for up to 24 h and then decreased sharply (Fig. 5d). In our previous studies, the first version of the peptide (namely LRG1 BP3) had a much lower stability of up to 3 h only; however, our engineered peptides were quite stable for 24 h. This result is interesting because the re-engineered peptides used in this experiment were much more stable than the first version of the peptides [3]. We have previously identified unique peptides which are specific for LRG1 protein and characterized for the first time in the use of peptide bioreceptor for biosensor development [3]. To improve their binding characteristics, a database of peptide sequence combined with bioinformatics-based molecular prediction was carried out. Using these approaches, the peptides with increased binding performance including stability was successfully developed. We also tested the accuracy of the developed sensor. The sensor response and reproducibility with SWV were shown in Table S2. As expected, the most of coefficient of variation (COV) was below 12%, suggesting that this sensor is highly reproducible and accurate for the detection of LRG1.

3.8. Quantification of LRG1 in spiked human plasma sample

The presence of cancer in the body can be detected at an early stage using some biomolecules or processes in the body, defined as biomarkers. Among these, several blood biomarkers have been reported to be able to distinguish between various diseases, including cancer. As a biomarker for screening CRC, LRG1 protein is secreted into blood, enabling its early diagnosis [1]. Therefore, it is necessary to confirm whether our peptide-based electrochemical sensor can detect the LRG1 protein in actual blood or plasma samples. The complexity of biological samples can affect the structure and biological binding of peptides and induce non-specific binding to gold surfaces. Therefore, the detection performance of the peptide for LRG1 in human plasma samples with complexed matrix should be confirmed. As mentioned above, our sensor showed a linear correlation in the range of 0.025−0.5 μg/mL. Therefore, commercially available human plasma was made a 10-fold serial dilution with distilled water, and then spiked with LRG1 protein at various concentrations (0.01−2.5 μg/mL). Then, the LRG1 BP3-2 immobilized gold electrode was reacted with the spiked sample, and the values before and after addition were compared to confirm whether the prepared sensor could quantitatively detect LRG1 in the samples (Fig. 6a). Our sensor showed an average recovery of 101.2% at 0.01 and 0.1 μg/mL, which indicated efficient detection of the LRG1 protein in the plasma sample (Table S3). As shown in Table S3, the coefficient of variation (COV) in

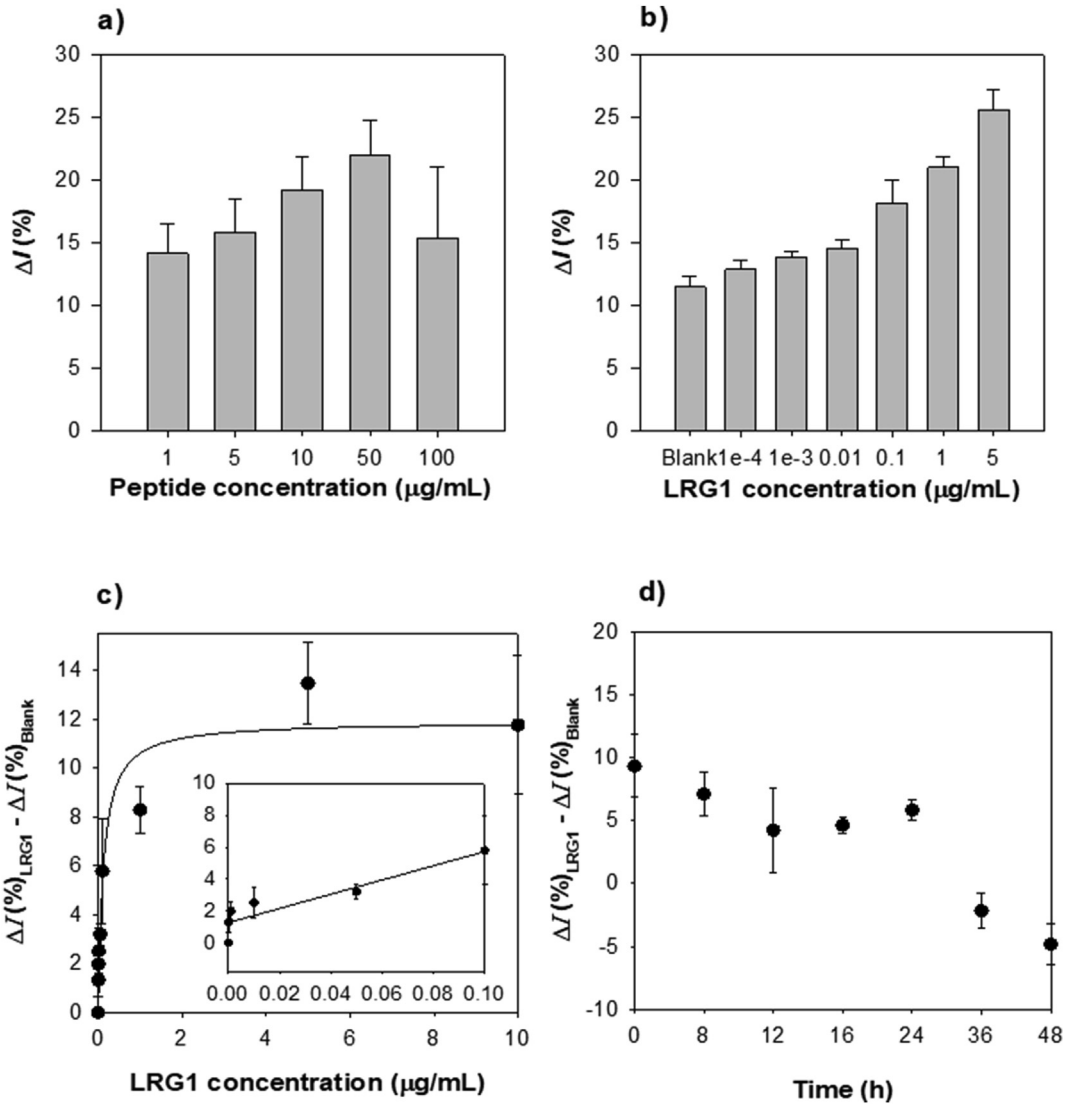

Fig. 5. Optimization and characterization of the selected peptides. a) Effects of BP3-2 peptide concentrations on the binding interactions, b) Effects of LRG1 protein concentration on the binding interactions, c) Determination of dissociation constant (K_d), d) Stability of the sensor system. All measurements were taken in triplicate; error bars represent standard deviations.

SWV measurement was ranged from 2% to 11% with relative recovery (31.68−101.57).

To evaluate the feasibility of the developed sensor, a total of 10 patient samples were serially diluted 100-fold and put on the sensor layer. The measured Δ*I* values for the two groups are shown in Fig. 6b. In our sensor, the mean Δ*I* values for adenoma and carcinoma were found to be 19.93 and 30.43, respectively. The two-tailed *p*-value ($p = 0.006$) and the one-tailed *p*-value ($p = 0.003$) of the *t*-test showed a significant difference. We also calculated the LRG1 concentration in all tested samples (Table S4). As shown in Table S4, the average measured LRG1 concentration in the adenoma and carcinoma was found to be 25.61 μg/mL and 39.79 μg/mL, respectively. This is close to the normal level of LRG1 in adenoma (~36.6 μg/mL) and carcinoma (~60.6 μg/mL) [1]. The comparison of detection performance between commercially available ELISA assay kit and our sensor was summarized in Table S5.

4. Conclusion

In CRC, it is crucial to distinguish between adenoma and carcinoma. Therefore, in this study, we designed improved affinity peptides for an advanced electrochemical sensor for identifying the adenoma to carcinoma transition, which would be useful in point-of-care testing. To increase the sensitivity, stability, and reproducibility of the sensor, eight peptides with different linkers were rationally designed by *in silico* modeling and were chemically synthesized, and a new specific immobilization method using aromatic rings was developed. Using SWV measurement, the LRG1 BP3-2 peptide was selected as it showed the highest affinity for LRG1 protein, a potential biomarker in colon cancer. Our newly designed peptide LRG1 BP3-2 with an optimized immobilization method, demonstrated significantly improved reproducibility and stability compared to our previously reported peptide. In the biosensing field, the dynamic detection range for the target of interest is important to exactly quantify the target. This allows reproducible and precise outcome. With these considerations, our developed electrochemical sensor exhibited lower detection ranging from 0.025 to 0.5 μg/mL of LRG1 protein. The LRG1 level in the blood of colon cancer patients was found to be around 10 μg/mL or lower. Thus, the reported sensor is promising for application in real point-

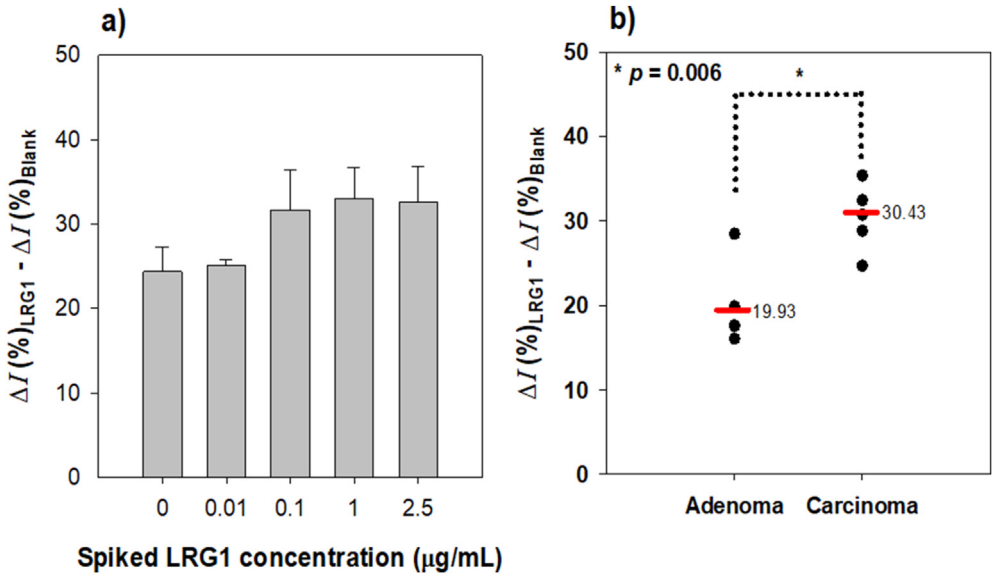

Fig. 6. Electrochemical sensor operation. a) Detection performance using spiked samples, b) Detection performance using plasma from patients with CRC.

of-care testing over the conventional ELISA. We confirmed that this sensor could detect the LRG1 protein in spiked human plasma samples without any cross-reactivity. We also found that the developed sensor showed 102% recovery, ranging from 0.01 to 0.1 μg/mL. These results indicate that our sensor efficiently detects LRG1 protein and can be used in clinical practice. Compared to the antibody-based immunoassay, this electrochemical sensor system offers several advantages, including easy operation and short analysis time. Therefore, our peptide-based sensor can be a cost-effective and convenient strategy for discriminating adenomas and carcinomas of CRC or for developing sensors to diagnose various diseases, and can be used in various biomedical and clinical fields.

Declaration of competing interest

The authors declare that they have no known competing financial interests or personal relationships that could have appeared to influence the work reported in this paper.

Acknowledgments

This study was supported by a National Research Foundation of Korea (NRF) grant funded by the Korea government (MSIP) (NRF-2017R1A2A2A05001037, NRF-2019R1A2C2084065).

Appendix A. Supplementary data

Supplementary data to this article can be found online at https://doi.org/10.1016/j.aca.2020.11.011.

Credit Author Statement

CH Cho, JH Kim, TJ Park, JP Park: conceived and designed the experiments.

CH Cho, JH Kim, J Kim, JW Yun, TJ Park, JP Park: performed the experiment and contributed to interpretation of the data.

CH Cho, JH Kim, TJ Park, JP Park: wrote paper.

References

[1] J.W. Choi, H. Liu, D.H. Shin, G.I. Yu, J.S. Hwang, E.S. Kim, J.W. Yun, Proteomic and cytokine plasma biomarkers for predicting progression from colorectal adenoma to carcinoma in human patients, Proteomics 13 (15) (2013) 2361–2374.

[2] H.J. Hwang, M.Y. Ryu, G.B. Lee, J.P. Park, Selection of high affinity peptides for prediction of colorectal adenoma-to-carcinoma progression, Chemistry 1 (6) (2016) 1140–1143.

[3] J.M. Lim, M.Y. Ryu, J.W. Yun, T.J. Park, J.P. Park, Electrochemical peptide sensor for diagnosing adenoma-carcinoma transition in colon cancer, Biosens, Bioelectron 98 (2017) 330–337.

[4] F. Bray, J. Ferlay, I. Soerjomataram, R.L. Siegel, L.A. Torre, A. Jemal, Global cancer statistics 2018: GLOBOCAN estimates of incidence and mortality worldwide for 36 cancers in 185 countries, CA A Cancer J. Clin. 68 (6) (2018) 394–424.

[5] J.H. Chik, J. Zhou, E.S. Moh, R. Christopherson, S.J. Clarke, M.P. Molloy, N.H. Packer, Comprehensive glycomics comparison between colon cancer cell cultures and tumours: implications for biomarker studies, J. Proteom. 108 (2014) 146–162.

[6] O. Galamb, F. Sipos, S. Spisak, B. Galamb, T. Krenacs, G. Valcz, Z. Tulassay, B. Molnar, Potential biomarkers of colorectal adenoma-dysplasia-carcinoma progression: mRNA expression profiling and in situ protein detection on TMAs reveal 15 sequentially upregulated and 2 downregulated genes, Cell. Oncol. 31 (1) (2009) 19–29.

[7] L. Giusti, P. Iacconi, Y. Da Valle, F. Ciregia, T. Ventroni, E. Donadio, G. Giannaccini, M. Chiarugi, L. Torregrossa, A. Proietti, F. Basolo, A. Lucacchini, A proteomic profile of washing fluid from the colorectal tract to search for potential biomarkers of colon cancer, Mol. Biosyst. 8 (4) (2012) 1088–1099.

[8] T.F. Imperiale, D.F. Ransohoff, S.H. Itzkowitz, T.R. Levin, P. Lavin, G.P. Lidgard, D.A. Ahlquist, B.M. Berger, Multitarget stool DNA testing for colorectal-cancer screening, N. Engl. J. Med. 370 (14) (2014) 1287–1297.

[9] S. Kumar, J.R. Dimmock, R.K. Sharma, The potential use of N-myristoyltransferase as a biomarker in the early diagnosis of colon cancer, Cancers 3 (1) (2011) 1372–1382.

[10] K. Rangiah, M. Tippornwong, V. Sangar, D. Austin, M.P. Tetreault, A.K. Rustgi, I.A. Blair, K.H. Yu, Differential secreted proteome approach in murine model for candidate biomarker discovery in colon cancer, J. Proteome Res. 8 (11) (2009) 5153–5164.

[11] R.E. Schoen, The case for population-based screening for colorectal cancer, Nat. Rev. Canc. 2 (2002).

[12] X. Sole, M. Crous-Bou, D. Cordero, D. Olivares, E. Guino, R. Sanz-Pamplona, F. Rodriguez-Moranta, X. Sanjuan, J. de Oca, R. Salazar, V. Moreno, Discovery and validation of new potential biomarkers for early detection of colon cancer, PLoS One 9 (9) (2014), e106748.

[13] J.A. Webb, R. Bardhan, Emerging advances in nanomedicine with engineered gold nanostructures, Nanoscale 6 (5) (2014) 2502–2530.

[14] L. Wu, X. Qu, Cancer biomarker detection: recent achievements and challenges, Chem. Soc. Rev. 44 (10) (2015) 2963–2997.

[15] J.M. Yi, M. Dhir, A.A. Guzzetta, C.A. Iacobuzio-Donahue, K. Heo, K.M. Yang, H. Suzuki, M. Toyota, H.M. Kim, N. Ahuja, DNA methylation biomarker candidates for early detection of colon cancer, Tumour Biol 33 (2) (2012) 363–372.

[16] Y. Zhang, J. Chen, Z. Hu, D. Hu, Y. Pan, S. Ou, G. Liu, X. Yin, J. Zhao, L. Ren, J. Wang, Panning and identification of a colon tumor binding peptide from a phage display peptide library, J. Biomol. Screen 12 (3) (2007) 429–435.
[17] T. Li, M.H. Leong, B. Harms, G. Kennedy, L. Chen, MicroRNA-21 as a potential colon and rectal cancer biomarker, World J. Gastroenterol. 19 (34) (2013) 5615–5621.
[18] A. Kume, M. Okochi, K. Shimizu, Y. Yoshida, H. Honda, Development of a tactical screening method to investigate the characteristics of functional peptides, Biotechnol. Bioproc. Eng. 21 (1) (2016) 119–127.
[19] J.M. Lim, M.Y. Ryu, J.H. Kim, C.H. Cho, T.J. Park, J.P. Park, An electrochemical biosensor for detection of the sepsis-related biomarker procalcitonin, RSC Adv. 7 (58) (2017) 36562–36565.
[20] W. Shao, W. Zhu, Y. Wang, J. Lu, G. Jin, Y. Wang, W. Su, Rational design and molecular engineering of peptide aptamers to target human pancreatic trypsin in acute pancreatitis, Biotechnol, Bioprocess Eng. 21 (1) (2016) 144–152.
[21] D. Wu, G. Li, C. Qin, X. Ren, Phage displayed peptides to avian H5N1 virus distinguished the virus from other viruses, PLoS One 6 (8) (2011), e23058.
[22] J.M. Lim, M.Y. Ryu, J.W. Yun, T.J. Park, J.P. Park, Electrochemical peptide sensor for diagnosing adenoma-carcinoma transition in colon cancer, Biosens, Bioelectron 98 (2017) 330–337.
[23] J.H. Lee, B. Fan, T.D. Samdin, D.A. Monteiro, M.S. Desai, O. Scheideler, H.-E. Jin, S. Kim, S.-W. Lee, Phage-based structural color sensors and their pattern recognition sensing system, ACS Nano 11 (4) (2017) 3632–3641.
[24] S.S. Sidhu, Engineering M13 for phage display, Biomol. Eng. 18 (2) (2001) 57–63.
[25] J. Wu, J.P. Park, K. Dooley, D.M. Cropek, A.C. West, S. Banta, Rapid development of new protein biosensors utilizing peptides obtained via phage display, PLoS One 6 (10) (2011), e24948.
[26] T. Matsubara, D. Ishikawa, T. Taki, Y. Okahata, T. Sato, Selection of ganglioside GM1-binding peptides by using a phage library, FEBS Lett. 456 (2) (1999) 253–256.
[27] J.P. Park, C.Y. Park, A.Y. Park, M.Y. Ryu, Evolutionary identification of affinity peptides for the detection of sepsis biomarker procalcitonin, RSC Adv. 5 (110) (2015) 90531–90533.
[28] H.J. Hwang, M.Y. Ryu, J.P. Park, Identification of high affinity peptides for capturing norovirus capsid proteins, RSC Adv. 5 (68) (2015) 55300–55302.
[29] C.H. Cho, J.H. Kim, D.K. Song, T.J. Park, J.P. Park, An affinity peptide-incorporated electrochemical biosensor for the detection of neutrophil gelatinase-associated lipocalin, Biosens. Bioelectron. 142 (2019) 111482.
[30] Y.S. Grewal, M.J.A. Shiddiky, L.J. Spadafora, G.A. Cangelosi, M. Trau, Nano-yeast-scFv probes on screen-printed gold electrodes for detection of Entamoeba histolytica antigens in a biological matrix, Biosens. Bioelectron. 55 (2014) 417–422.
[31] H.J. Hwang, M.Y. Ryu, C.Y. Park, J. Ahn, H.G. Park, C. Choi, S.-D. Ha, T.J. Park, J.P. Park, High sensitive and selective electrochemical biosensor: label-free detection of human norovirus using affinity peptide as molecular binder, Biosens. Bioelectron. 87 (2017) 164–170.
[32] J.M. Lim, N.S. Heo, S.Y. Oh, M.Y. Ryu, J.H. Seo, T.J. Park, Y.S. Huh, J.P. Park, Selection of affinity peptides for interference-free detection of cholera toxin, Biosens. Bioelectron. 99 (2018) 289–295.
[33] D. Lee, J. Hwang, Y. Seo, A.A. Gilad, J. Choi, Optical immunosensors for the efficient detection of target biomolecules, Biotechnol. Bioproc. Eng. 23 (2) (2018) 123–133.
[34] S.G. Meirinho, L.G. Dias, A.M. Peres, L.R. Rodrigues, Electrochemical aptasensor for human osteopontin detection using a DNA aptamer selected by SELEX, Anal. Chim. Acta 987 (2017) 25–37.
[35] M. Nuzaihan, M.N.U. Hashim, M.K. Md Arshad, S.R. Kasjoo, S.F.A. Rahman, A.R. Ruslinda, M.F.M. Fathil, R. Adzhri, M.M. Shahimin, Electrical detection of dengue virus (DENV) DNA oligomer using silicon nanowire biosensor with novel molecular gate control, Biosens. Bioelectron. 83 (2016) 106–114.
[36] Z. Su, H. Xu, X. Xu, X. Xu, Y. Zhang, Y. Ma, C. Yi, Q. Xie, Effective covalent immobilization of quinone and aptamer onto a gold electrode via thiol addtiion for sensitive and selective protein biosensing, Talanta 164 (2017) 244–248.
[37] D. Qu, B.C. Kim, C.W. Lee, M. Ito, H. Noguchi, K. Uosaki, 1,6-hexanedithiol self-assembled monolayers on Au(111) investigated by electrochemical, spectroscopy, and molecular mechanics methods, J. Phys. Chem. 114 (2010) 497–505.
[38] C. Vericat, M.E. Vela, G. Benitez, P. Carro, R.C. Salvarezza, Self-assembled monolayers of thiols and dithiols on gold: new challenges for a well-known system, Chem. Soc. Rev. 39 (2010) 1805–1834.